

EVALUATION OF THE HEALING OF WOUNDS DRESSED WITH ZINC METAL-ORGANIC FRAMEWORKS (ZN-MOFS) IN DOGS: AN EXPERIMENTAL STUDY

REHAM M. ABD-EL AZEEM ¹; AHMED IBRAHIM ²; MOHAMED H. KOTOB ³; ABDELNABY ELSHAHAWY ⁴ AND SAMIA M. SELIM ⁵

¹ B.V.Sc., Assiut University, Assiut, Egypt

² Veterinary Teaching Hospital, Faculty of Veterinary Medicine, Assiut University, Assiut, Egypt, Email: elgrah38@gmail.com

³ Department of Pathology and Clinical Pathology, Faculty of Veterinary Medicine, Assiut University, Assiut, Egypt, Email: mohammedkotob@yahoo.com

⁴ Department of Physics, Faculty of Science, Assiut University, Assiut, Egypt, Email: a.elshahawy97@gmail.com

⁵ Department of Surgery, Anesthesiology, and Radiology, Faculty of Veterinary Medicine, Assiut University, Assiut, Egypt

Received: 24 August 2022; **Accepted:** 8 September 2022

ABSTRACT

This study aimed to evaluate the healing of wounds dressed with Zn-MoF in dogs. The study was conducted on fifteen clinically healthy mongrel dogs. Each dog has bilateral cutaneous excisional wounds (2×2 cm²). Right-side wounds were dressed with Zn-MOF dressing (treated wounds) under the effect of 1 mg/kg of xylazine HCL 2% and 10 mg/kg of ketamine HCL 5% , administered in one syringe intramuscularly (IM), while left-side wounds were dressed with normal saline (control group). Wounds were undergone to histopathological evaluation 7-, 15-, and 21-days post-wound induction (5 dogs each interval). Zn-MOF positively enhanced the re-epithelization of the wound area promoting the epidermal hyperplasia resulting in reduction of the wound size and epithelial gap that was completely closed and restored on day 21 post-wound induction. The control wounds were at a slower healing rate with time leaving epithelial gaps and did not completely close day 21 post-wound induction. Zn-MOF treated wounds' dermis was pervaded with the inflammatory cells on day 7 post-wound induction that gradually reduced by time and replaced by fibroblasts 14- and 21-days post-wound induction. The dermis of control wounds was severely infiltrated with a larger number of inflammatory cells and excessive hemorrhage throughout the study. Zn-MOF treated wounds had an augment in the number and size of newly formed blood vessels in comparison to the control ones, reaching their highest point on day 14- and declining on day 21 post-wound induction. Collagen deposition increased obviously 21 days post-wounding in Zn-MOF treated wounds. Zn-MOF accelerated and enhanced the wound healing process and abundant granulation tissue formation in dogs.

Key words: Zinc, Zn-MOF, wound, healing, dogs.

Corresponding author: Reham M. Abd-El Azeem

E-mail address: az4524311@gmail.com

Present address: B.V.Sc., Assiut University, Assiut, Egypt

INTRODUCTION

Wound healing is a natural physiological process that occurs as a response to any injury to the tissue. Wounds have variable causes involving injuries, burns, and pathological conditions such as diabetes or vascular diseases. Wounds are classified into acute or chronic wounds according to their underlying causes and consequences (Karimi *et al.*, 2017).

Successful wound management depends on understanding the healing process, as well as the properties of the various dressing materials to maximize the treatment efficiency (Weller and Sussman, 2006).

Zinc is an essential trace element and a vital micronutrient for the function of more than 10% of metalloenzymes/proteins required for cell membrane repair, cell proliferation, growth, and immune system function. Therefore, zinc deficiency can cause impairment in immune function and wound healing (Lin *et al.*, 2017; Soliman, 2005).

Metal organic frameworks (MOFs) are among nanotechnology's most developing strategies that have been published in the last ten years (Hinks *et al.*, 2010). MOFs are a group of crystalline, hybrid, coordinating materials made up of inorganic clusters (metal ions) connected by organic polydentate ligands/linkers (Yu *et al.*, 2018). Currently, MOFs are getting wider attention for wound healing due to their increased drug loading capacity, controlled release of the agents/products of wound healing, lesser toxicity profile, natural angiogenic and antibacterial

features in comparison to other traditional nanomaterials (Xiao *et al.*, 2017; Chen *et al.*, 2019; Zhang S. *et al.*, 2020; Zhang M. *et al.*, 2020). Zinc can be used as a central block of MOFs, which helps in the healing of wounds through its enhancement effect on proliferation of cells, collagen build-up and angiogenesis (Hinks *et al.*, 2010; Rubin *et al.*, 2018; Hou and Tang, 2019; Kargozar *et al.*, 2019; Yao *et al.*, 2020).

Recent studies demonstrated the potential of zn-based MOFs as practical drug delivery system, nontoxic, and biocompatible therapeutic agents in the biological and medical applications (Kitagawa *et al.*, 2004; Rezwani *et al.*, 2006; Ye *et al.*, 2015). However, current literature lacks reports regarding use of Zn-MOF dressing for wound treatment in dogs. Therefore, this study aimed to evaluate the healing of cutaneous excisional wounds dressed with Zn-MOF dressing in dogs.

MATERIALS AND METHODS

Ethical approval

The National Ethical Committee of the Faculty of Veterinary Medicine, Assiut University, Assiut, Egypt, has approved all the procedures in this study in accordance with the Egyptian bylaws and OIE animal welfare standards for animal care and use in research and education.

Zinc-MOF(Metal-organic frameworks) preparation

An appropriate amount of methylimidazole (2-MIM) was dissolved in 40 ml DI water and marked as a solution (A), another 2 mmol of Zn nitrate was added to 40 ml DI water and named as a solution (B). Solution (B) was then poured into solution (A) and stirred for a few seconds. 5 cm x 5 cm carbon cloth was immersed immediately into the

mixture and aged for 4 hours. The carbon cloth was then taken out and washed with (deionized water) then dry it in the drying oven (DHG-9075A) at 60 °C overnight (Figure 1). Field-emission scanning electron microscopy (SUPRA 40 ZEISS, Germany) in the electron microscopy unit,

Assiut University, was employed to examine the morphology, the distribution of Zn-MOF particles on the carbon cloth fibers, and then investigate the elemental distribution using Energy Dispersive Spectroscopy (EDX) (Hoop *et al.*, 2017).



Figure 1: Zn-MOF carbon mesh wound dressing.

Experimental animals

This study was conducted on fifteen ($n = 15$) clinically healthy mongrel dogs of both sexes (7 males and 8 non-pregnant, non-lactating females), weighing (13 – 15 kg), and aged 2 – 3 years. Dogs were kept in individual cages with ad libitum access to feed and water. Each dog has bilateral cutaneous excisional wounds ($2 \times 2 \text{ cm}^2$). Right-side wounds were dressed with Zn-MOF dressing (treated wounds, $n = 15$), while left-side wounds were dressed with normal saline (control groups, $n = 15$). Wounds were undergone to histopathological evaluation 7-, 15-, and 21-days post-wound induction (5 dogs each interval, $n = 5$).

Wound creation

Dogs were deprived of feed for 12 hours, but not for water. Wounds were conducted under the effect of 1 mg/kg of xylazine HCL 2% (Xyla-Ject, ADWIA Co., SAE, Egypt) and 10 mg/kg of

ketamine HCL 5% (Ketamine, Sigma-tec Pharmaceutical Industries, SAE, Egypt), administered in one syringe intramuscularly (IM). Dogs were positioned on the sternum, the bilateral areas of the midline were prepared for aseptic surgery; clipped, shaved, disinfected several times with betadine (BETADINE, El- Nile Co. for Pharmaceutical and Chemical Industries, Egypt), and draped except for the surgical site of wound creation. Using a sterile template, $2 \times 2 \text{ cm}^2$, full cutaneous excisional wounds were created bilaterally using a scalpel and scissors, 5 cm from the midline in the thorax region (Sardari *et al.*, 2006). (Figure 2A). Hemostasis was achieved by back pressure with sterile tampon of gauze. Wounds were digitally photographed with a sterile ruler included in the photos.

Right-side wounds were dressed with a sterile Zn-MOF mesh, while left-side

wounds were dressed with normal saline. Zn-MOF mesh was secured in situ by four interrupted stitches (Figure 2B). All wounds were covered by sterile cotton pad dressing, gauze, and elastic bandage. Dogs wore Elizabeth collar to keep them

away from wounds. Wound dressings were changed weekly. Dogs were administered pain medication, Carprofen (Rimadyl, 50 mg/ml, Zoetis), 4 mg/kg, intravenous (IV), daily for up to three successive days post-wound induction.

Day 0 post-wound induction

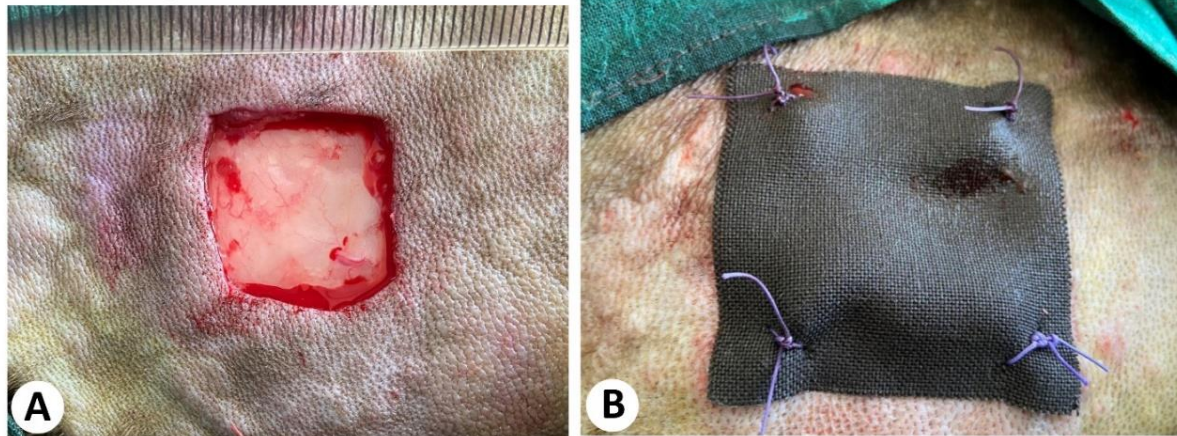


Figure 2: (A) 2×2 cm² full cutaneous excisional wound, (B) Zn-MOF mesh was secured in situ by four interrupted stitches.

Histopathological evaluation

Macroscopical evaluation

At each interval of wound evaluation (7-, 14-, and 21 days post-wound induction), wounds were grossly examined for the presence of abnormal signs e.g.: exudates, infection, or exuberant granulation tissues.

Planimetry of wounds

Each wound was photographed on days zero, one week, two weeks, and three weeks post-wound inductions. A standardized ruler was involved in each photograph to recognize the digital calibration of the photographs. pictures were taken after zooming on the shape of wounds. wound size's percentage was estimated by the ImageJ software analysis as described before by Sardari *et al.* (2009):

The wound size's percentage at day [x] compared to day [0] = the size of wound

at day [x] mm² / size of wound at day [0] mm² \times 100.

Microscopical evaluation

At the pre-determined interval of wound evaluation (7-, 14-, and 21 days post-wound induction) and under the effect of the same prescribed anesthetic protocol, tissue specimens were taken from the wounds for histopathological evaluation. Skin samples were collected from each dog and were fixed in 10% neutral buffered formalin. The formalin-fixed samples were proceeded in ascending grades of ethanol for dehydration, were cleared in Xylol, and then embedded in paraffin wax for sectioning. Paraffin sections were cut at 4 μ m in thickness and were stained with the following histological stains:

1. Ordinary Hematoxylin and Eosin stain for general histological examination (Fischer *et al.*, 2008).

2. Mc. Picrosirius red stain for collagen identification (Bhutda *et al.*, 2017).

The paraffin-stained sections were examined under a light microscope (Olympus, USA) by a histopathologist, who was blinded to the groups' arrangement and photos were taken by an Olympus DP72 camera adapted into the microscope. Newly formed blood vessels were counted in 5 images/wound sample

Wounds were left to recuperate following the harvesting of specimens for histopathological examination.

Statistical analysis

The values were introduced as Mean \pm standard deviation. The data were examined by one-way ANOVA using IBM SPSS statistics 20 (SPSS Inc., Chicago, IL, USA).

RESULTS

Clinical evaluation

Throughout the experiment the animals were alert, exhibiting normal activity, with normal access to feed and water. There were no recorded deaths.

Morphology and elemental analysis of Zn-MOF wound dressing

From the SEM images, 2D nano-wall configuration with thickness around 150 nm in an axis direction is confirmed as shown in Figure (3 A - C).

The energy dispersive X-ray images (EDX) in Figures (4 A & B, 5 A – C, and 6) show the elemental mapping for Zn-MOF on carbon cloth sample. The EDX images approves the successful conjugation of Zn cluster with the organic linker where Zn, O, C, and N are coexisted.

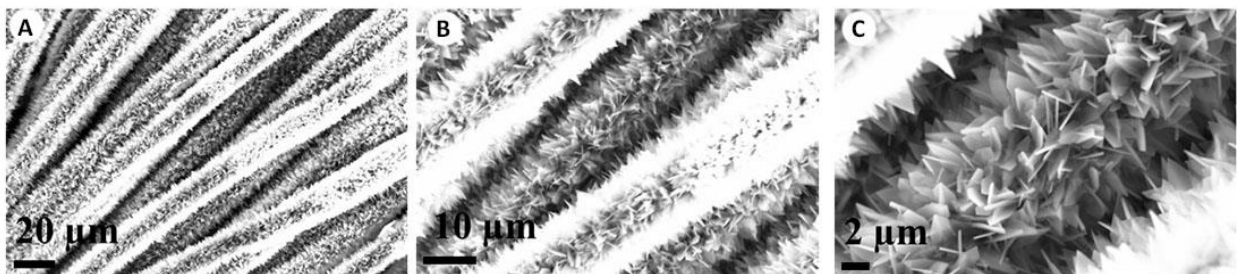


Figure 3: 2D nano-wall configuration with thickness around 150 nm in an axis direction.

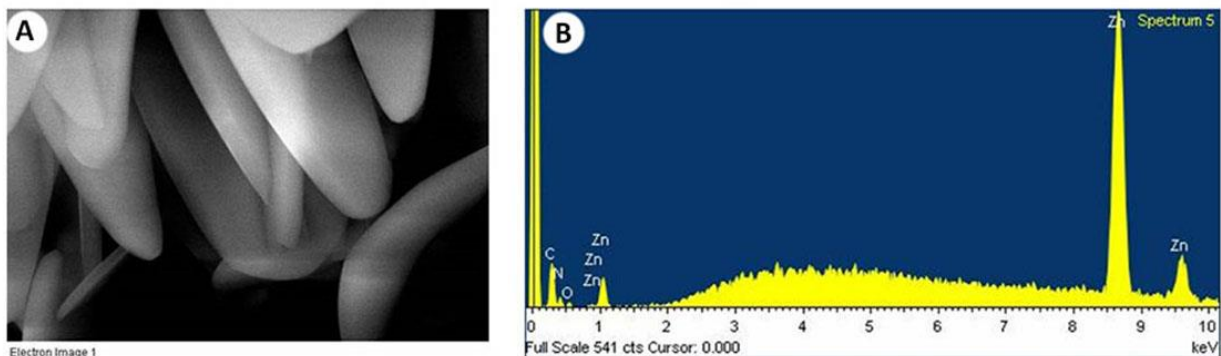


Figure 4: The energy dispersive X-ray images (EDX) showing the elemental mapping for Zn-MOF on the carbon cloth sample.

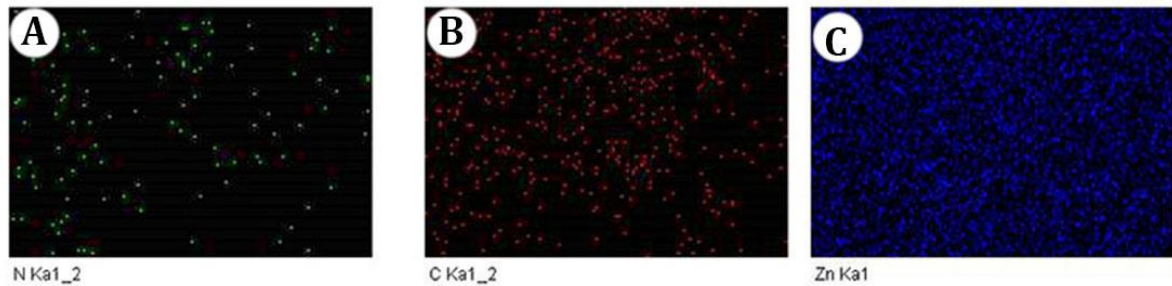


Figure 5: The energy dispersive X-ray images (EDX) showing the elemental mapping for Zn-MOF on the carbon cloth sample.

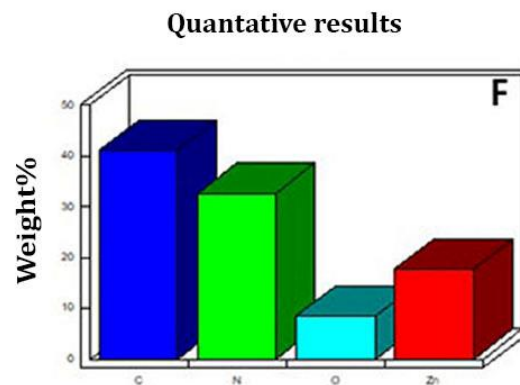


Figure 6: The energy dispersive X-ray images (EDX) showing the elemental mapping for Zn-MOF on the carbon cloth sample.

Histopathological evaluation

Gross evaluation of wounds

On day 7 post-wound induction, the wound started to cover with granulation tissue in both control and Zn-MOF treated wounds and the percentage of wound size reduction was non significantly different in both groups ($P < 0.05$) (Figure 7). It was also noticed presence of large amount of pus and smelly odor in the control wounds, while the treated ones showed less amount of pus. On day 14 post-wound induction, control wounds showed the presence of hyper-granulation tissue and a small amount of pus, while the Zn-MOF

treated ones showed signs of healing, a highly significant decrease in the wound size ($P < 0.0001$) compared to control ones (Figure 7) with less amount of granulation tissue and there was no pus or odor. On day 21 post-wound-induction, there were partial healing signs of control wounds, and the wounds were still covered with an unhealed scar with a lack of hair growth, while the treated wounds were healed and covered, the wound size was significantly decreased compared to control ones ($P < 0.05$) (Figure 7). Zn-MOF treated wounds showed new hair growth with no pus (Figure 8).

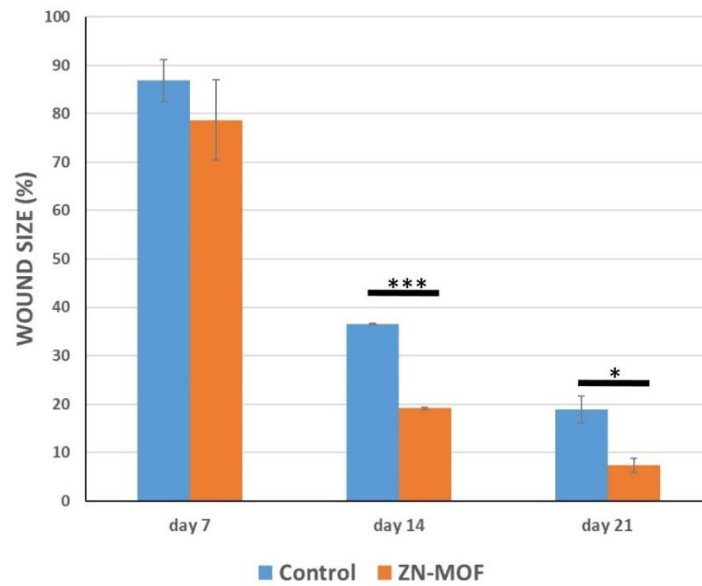


Figure 7: Planimetry of Zn-MOF treated- and control wounds 7-, 14-, and 21 days post wound induction in dogs.

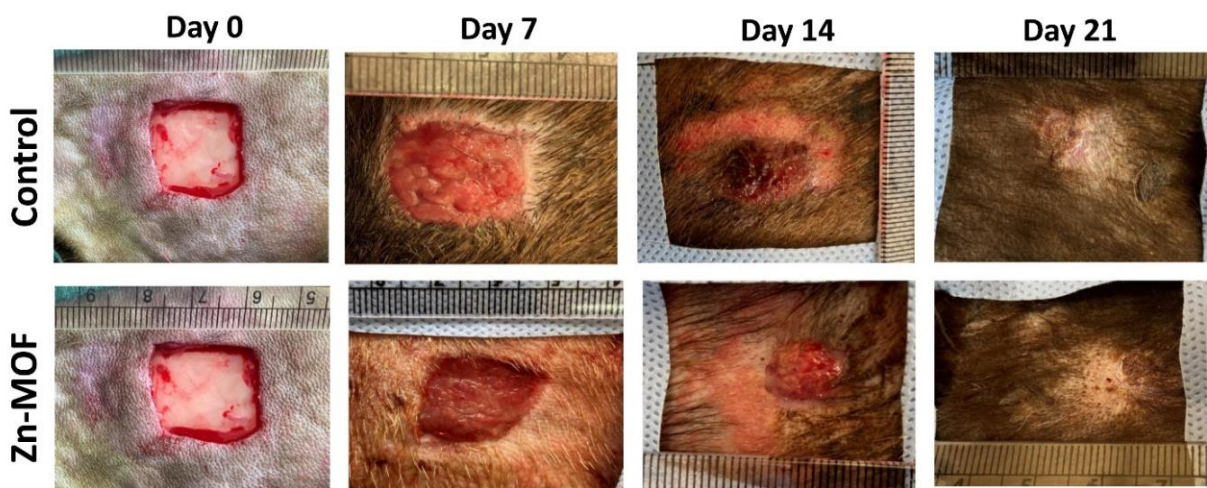


Figure 8: Gross examination of dorsal wounds in dogs treated with Zn-MOF or without. Representative photographs of the skin wounds of the control- or Zn-MOF treated wounds on days 0, 7, 14, and 21 post-wound inductions.

Microscopic examination:

On day 7 following the wound induction, there was no notable difference in the rate of wound healing and epithelization of the epidermis (20 % of wound size). Re-epithelization started at the wound edges but left a big epithelial gap in both control wounds and Zn-MOF treated wounds (Figure 9). Deposition of collagen fibers was more prominent in Zn-MOF treated wounds than in control ones (Figure 10).

The dermal layer in both groups was infiltrated with inflammatory cells (neutrophils and macrophages) and hemorrhages but Zn-MOF-treated wounds were characterized by a highly notable rise in the hyperemic new blood vessels' number ($P < 0.0001$) (Figure 11 A, B, D, E), (Figure 12). Destroyed hair follicles appeared in the dermis of control wounds but were normal in Zn-MOF treated ones (Figure 11 C, F).

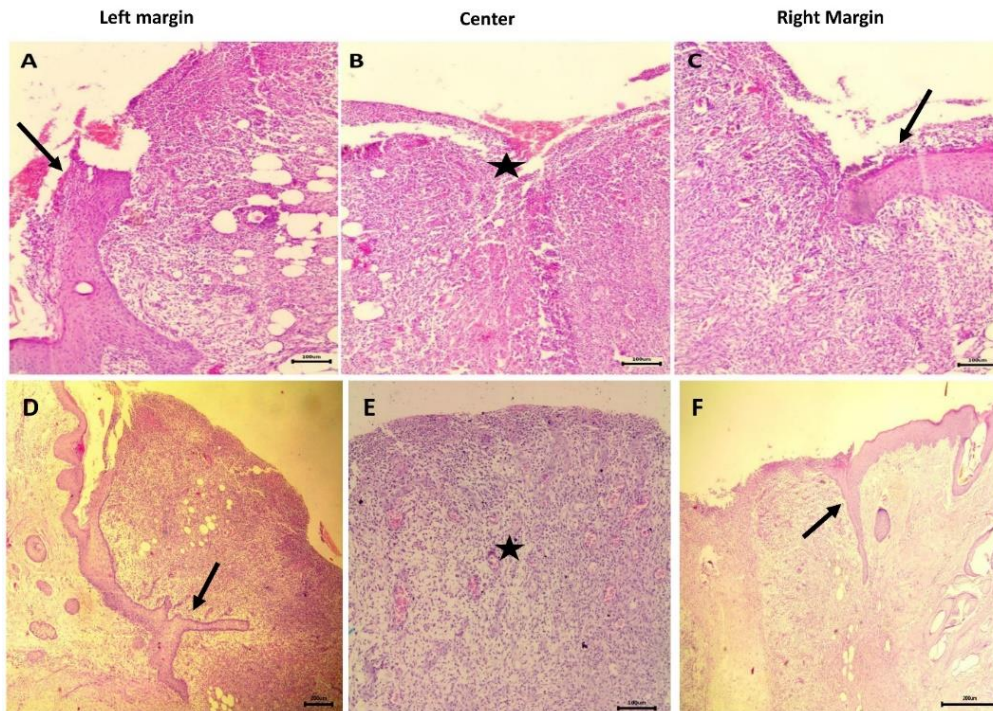


Figure 9: Micrographs of wound specimens on day 7 post-wound induction stained with hematoxylin and eosin stain. A, B, C control wounds, and D, E, F Zn-MOF treated wounds. The epithelization process started at the wound edges (arrow) and center of the wound was infiltrated with hemorrhage and inflammatory cells (star).

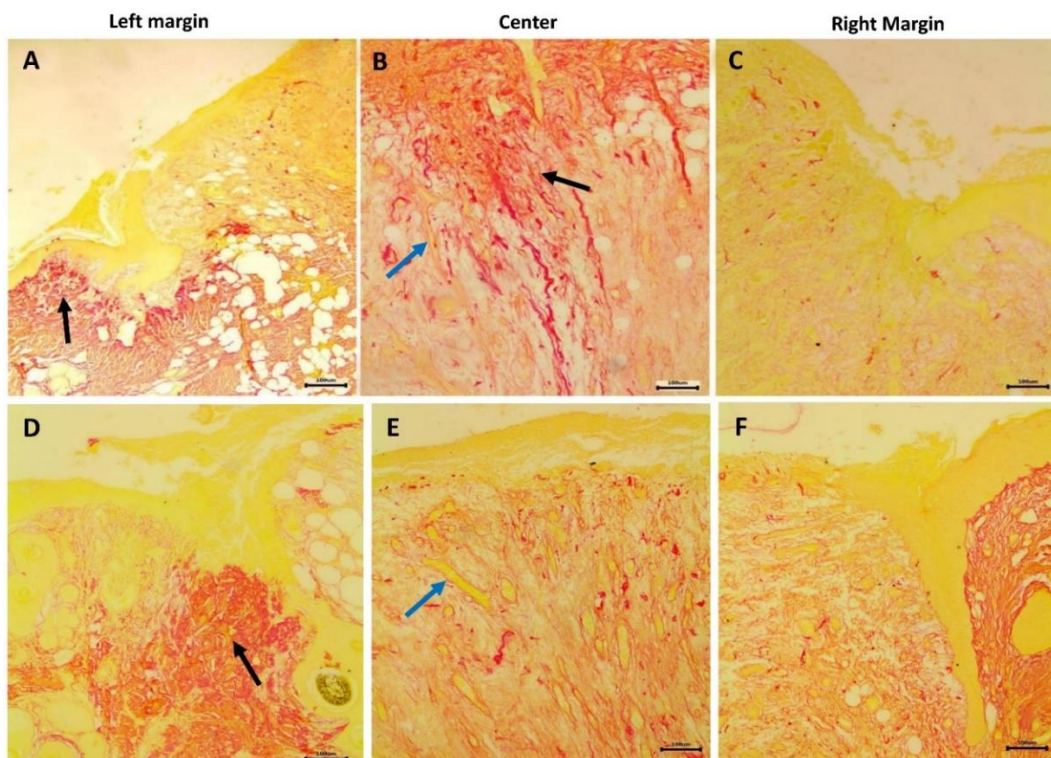


Figure 10: Micrographs of wound specimens on day 7 post-wound induction stained with Sirius red stain. A, B, C control wounds, and D, E, F Zn-MOF treated wounds. Deposition of red-stained collagen fibers (black arrow) and newly formed blood vessels (blue arrow) appeared in the dermal layer.

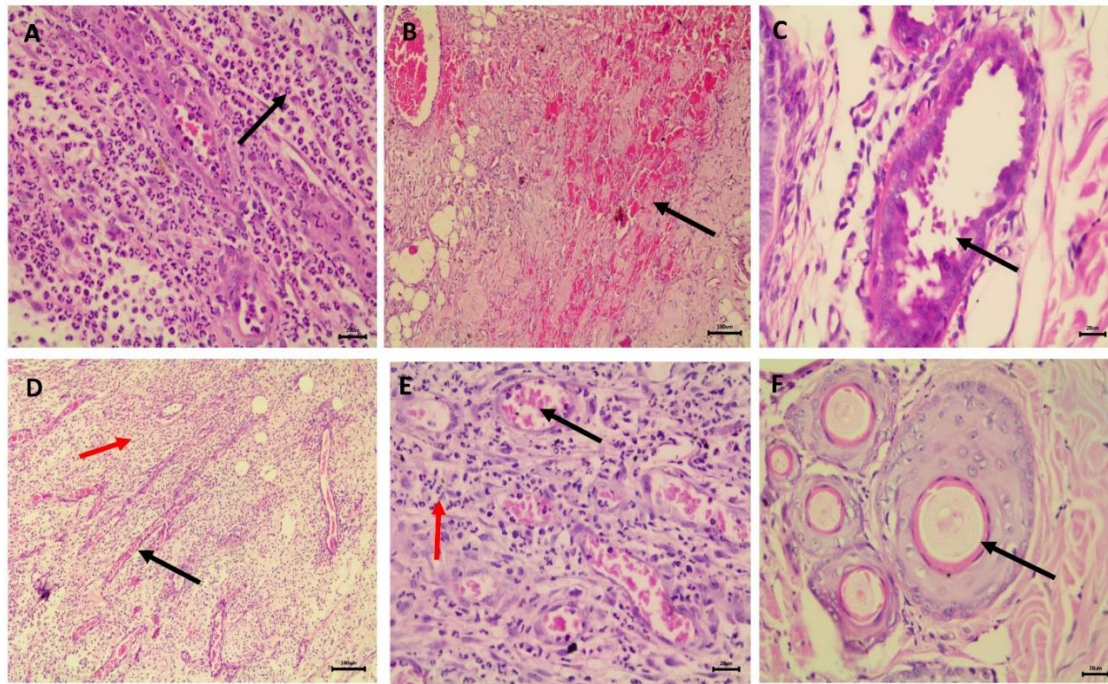


Figure 11: Micrographs of wound specimens on day 7 post-wound induction. A, B, C dermis of control wounds A: dermis infiltrated with a large number of neutrophils and macrophages; B: shows severe hemorrhage; C: demonstrates destroyed hair follicle. D, E, F dermis of Zn-MOF treated wounds D, E: show the presence of a large number of hyperemic large-sized new blood vessels (black arrow) and inflammatory cells (red arrow); F: shows normal non-destroyed hair follicle.

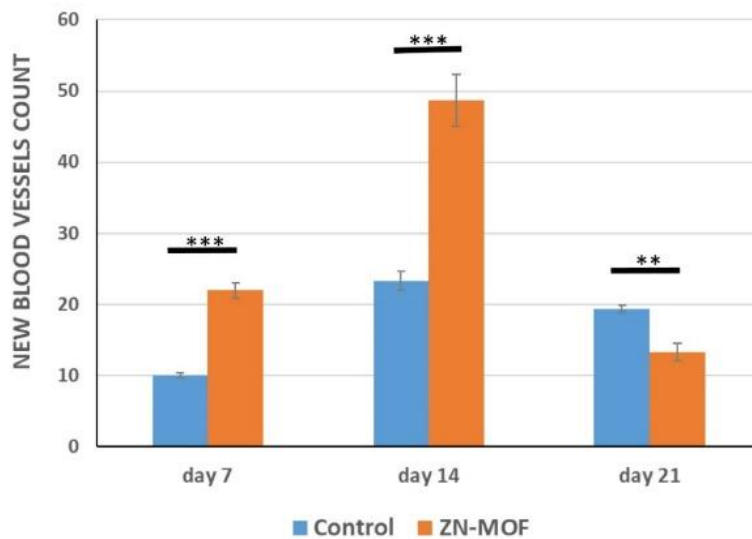


Figure 12: The number of hyperemic new blood vessels of Zn-MOF treated- and control wounds 7-, 14-, and 21 days post wound induction in dogs.

The healing process and re-epithelization of control wounds after 14 days were incomplete and reached 60 % of the

wound size left also a large epithelial gap with deposition of a small amount of collagenous fiber (Figures 13 and 14 A-

C). On the other side, the healing process of Zn-MOF treated wounds after 14 days was much better. The epithelization reached 80 % of the wound size and left a small epithelial gap and epidermal hyperplasia extended to the center of the wound (Figure 13 D-F). The collagen deposition was more pronounced and extended between the proliferating epidermis (Figure 14 D-F). The dermal layer was infiltrated with a great number of acute inflammatory cells (macrophages

and neutrophils or PMNL), extravasated red blood cells and a few newly formed blood capillaries. Destroyed hair follicles surrounded by inflammatory cells were seen (Figure 15 A, B). The dermal layer was infiltrated with a few acute inflammatory cells (neutrophils and macrophages), a highly significant increased number of new formed blood vessels ($P < 0.0001$) (Figure 12) and most of the hair follicles appeared normal in structure (Figure 15 C, D).

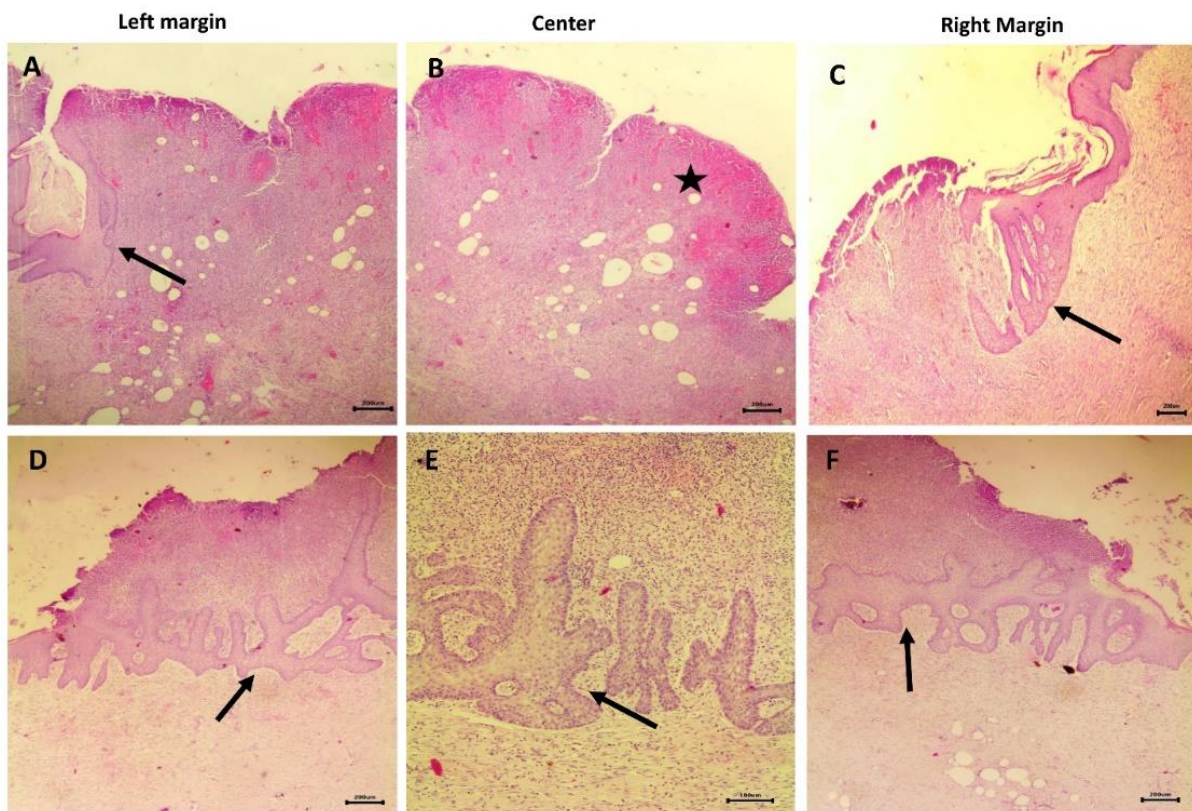


Figure 13: Micrographs of wound specimens on day 14 post-wound induction stained with hematoxylin and eosin stain. A, B, C control wounds showed increased epidermal hyperplasia toward center of the wound (arrow), excessive hemorrhage with severe inflammatory cell infiltration was still detected in center of the wound (star). D, E, F Zn-MOF treated wounds showed more pronounced epidermal hyperplasia extended toward center of the wound leaving a smaller epithelial gap (arrow) and the center showed less hemorrhage and inflammatory cell infiltration.

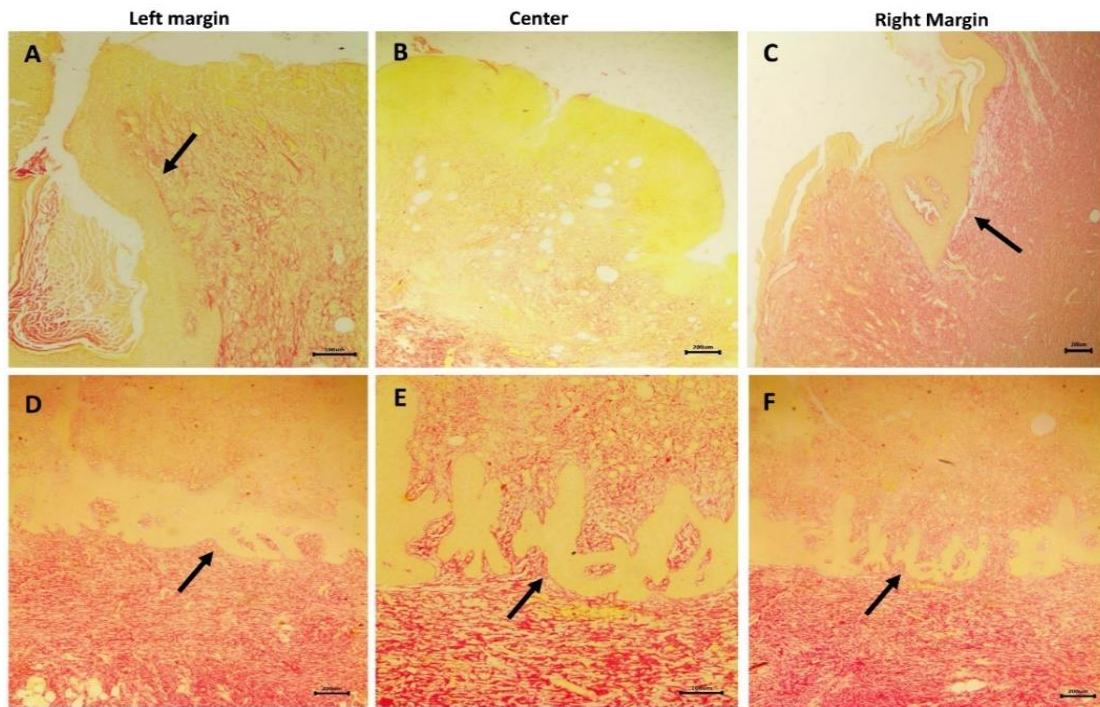


Figure 14: Micrographs of wound specimens on day 14 post-wound induction stained with Sirius red stain. A, B, C control wounds, and D, E, F Zn-MOF treated wounds. Deposition of red-stained collagen fibers was more prominent in Zn-MOF treated wounds than in control ones (arrow).

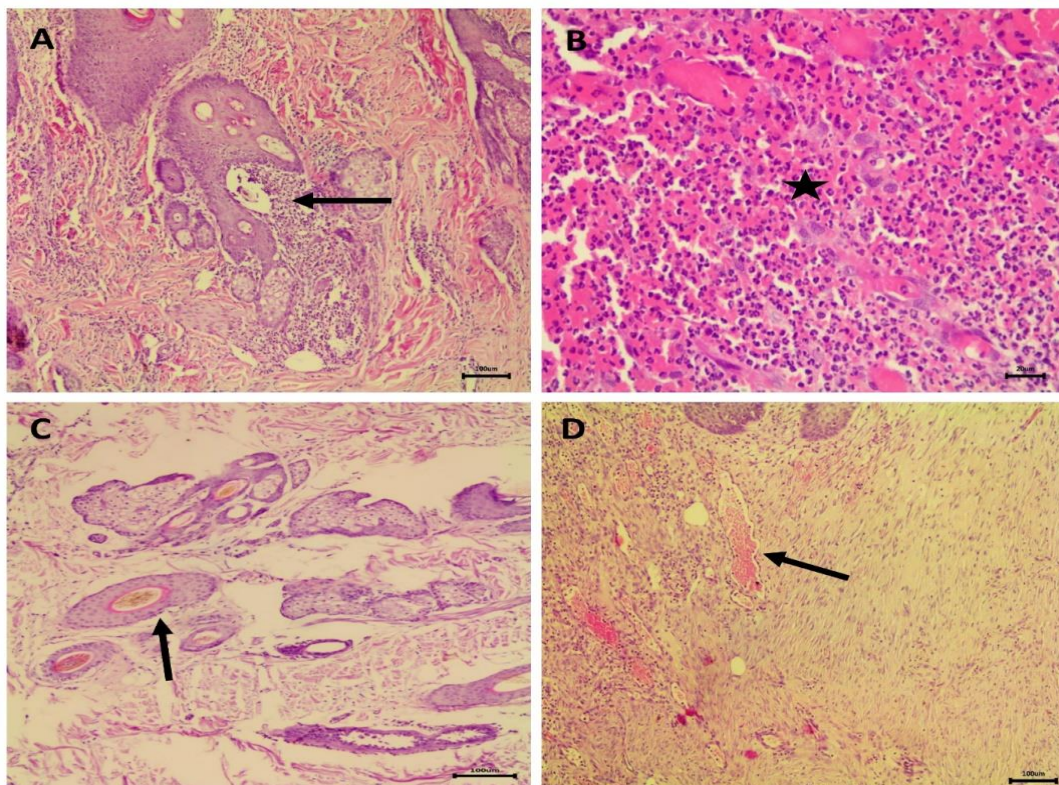


Figure 15: Micrographs of wound specimens on day 14 post-wound induction. A, B dermis of control wounds infiltrated with a large number of inflammatory cells, extravasated RBCs and a few newly formed blood vessels. C, D dermis of Zn-MOF treated wounds infiltrated with few inflammatory cells and a large number of hyperemic large-sized new blood vessels.

On day 21 post-wound induction the healing process of control wounds was not completed, and the wounds were not totally closed with the presence of a small epithelial gap between the epidermal edges that was covered with a scar formed of destroyed tissue and inflammatory cells (Figure 16 A-C). On the contrary, the healing of Zn-MOF treated wounds on day 21 was totally completed and the epithelization and tissue remodeling reached 100 % of the wound size. The wound was completely closed and healed with no epithelial gap and the scar was completely removed (Figure 16 D-F). The

collagen deposition of mature type on day 21 post-wound induction was more obvious in Zn-MOF treated wounds than in control ones (Figure 17). The dermal layer of the control wounds was still infiltrated with acute inflammatory cells, extravasated red blood cells and hyperemic new blood vessels (Figure 18 A, B). While the dermis of Zn-MOF treated ones was characterized by the dramatic significant decrease of newly formed blood vessels ($P < 0.001$) (Figure 12) and acute inflammatory cells and with the presence of newly formed hair follicles (Figure 18 C, D).

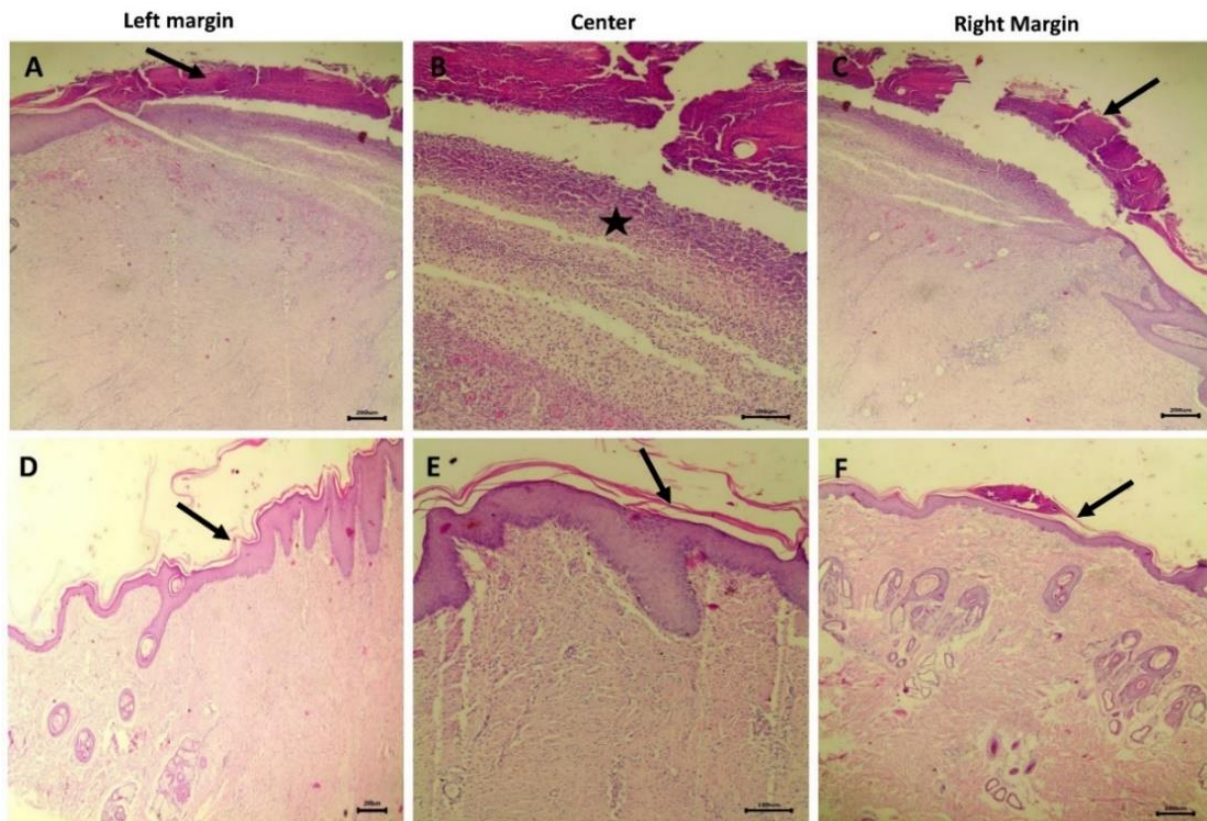


Figure 16: Micrographs of wound specimens on day 21 post-wound induction stained with hematoxylin and eosin stain. A, B, C control wounds showed not completed epithelization and a big epithelial gap covered with epithelial crust (arrow) and severe inflammatory cell infiltration in the dermal layer. D, E, F Zn-MOF treated wounds showed completely covered epidermis and no epithelial gap (arrow) and very few inflammatory cells and new blood vessels were detected in the dermal layer.

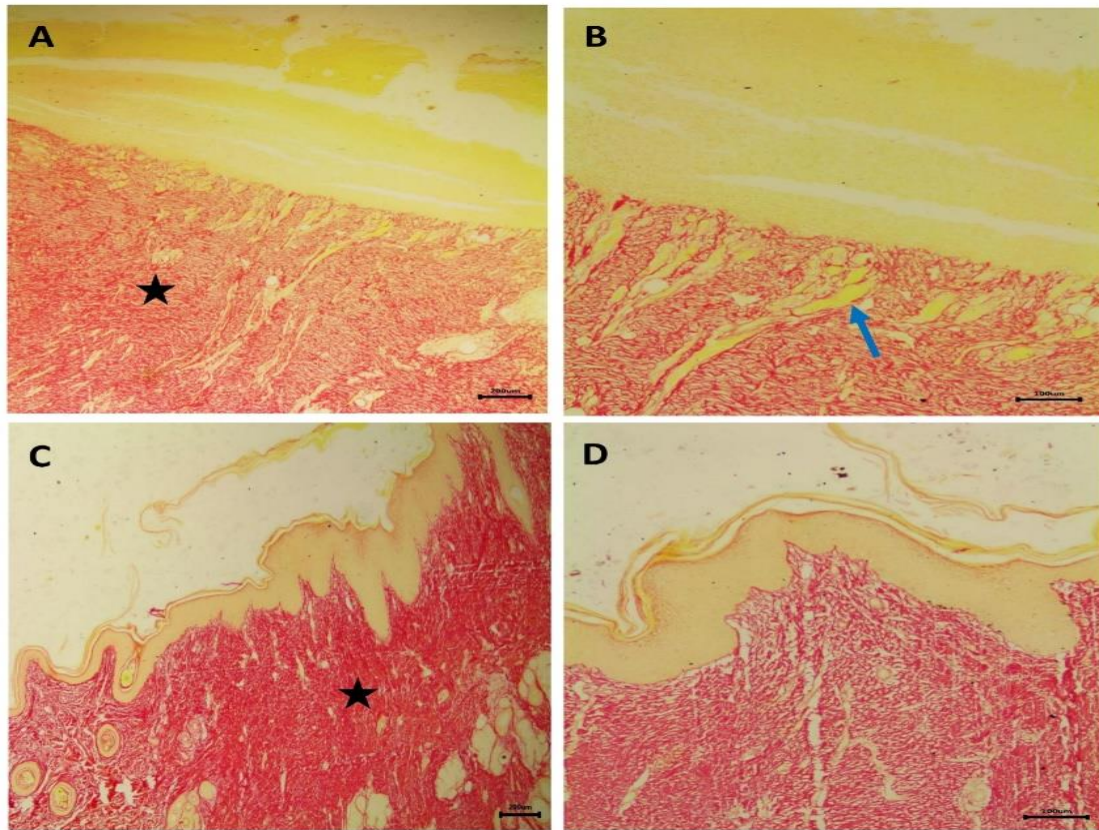


Figure 17: Micrographs of wound specimens on day 21 post-wound induction stained with Sirius red stain. A, B, control wounds, and C, D Zn-MOF treated wounds. Deposition of red-stained collagen fibers was more prominent in Zn-MOF treated wounds than in control ones (star). Newly formed blood vessels were more abundant in control wounds than Zn-MOF treated wounds (blue arrow).

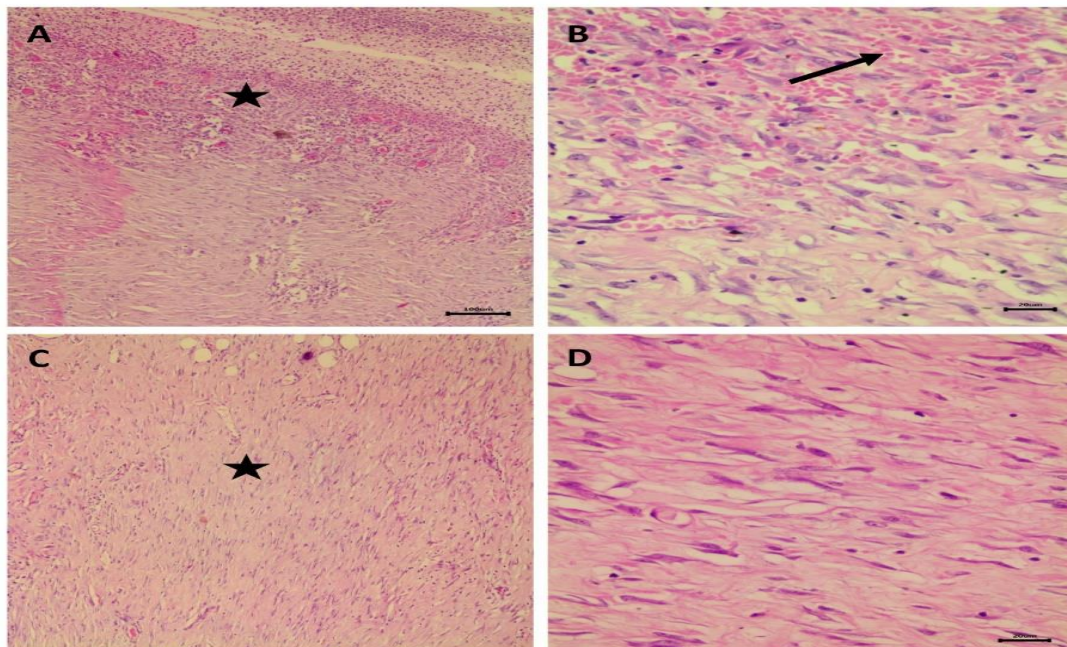


Figure 18: Micrographs of wound specimens on day 21 post-wound induction. A, B dermis of control wounds still infiltrated with inflammatory cells, extravasated RBCs and new blood vessels. C, D dermis of Zn-MOF treated wounds infiltrated with less inflammatory cells and very few new blood vessels.

DISCUSSION

Wound healing process depends on the interactions between different types of cells, coagulation factors, and growth factors (Singer and Clark, 1999; Gurtner *et al.*, 2008; Suarato *et al.*, 2018; Tottoli *et al.*, 2020). Wound healing pass through phases that activated by intra and intercellular pathways to restore tissue integrity. These phases include hemostasis, inflammation, proliferation, and remodeling phases (Martin, 1997; Regan and Barbul, 1999; Gurtner *et al.*, 2008; Bielefeld *et al.*, 2013; Das and Baker, 2016).

Any impairment during the sequence of the healing phases can lead to chronic wounds, with potential impacts on the quality of life (Suarato *et al.*, 2018). Wound persistence leads to the prolonged hospitalization time, as well as morbidity and even mortality (Ward *et al.*, 2019). Chronic wounds are mainly related to treatment and management strategies limiting the wound healing (Borena *et al.*, 2015). Therefore, several studies are conducted to achieve more effective wound treatments and reduce costs (Schiavon *et al.*, 2016).

Zinc is vital for metabolism, immunity, and healing process (Roohani *et al.*, 2013). Moreover, zinc-dependent proteins are important for DNA repair and apoptosis (Zheng *et al.*, 2015; Cho *et al.*, 2016), metabolic processing (Cronin and Walton, 2003),

extracellular matrix (ECM) regulation (Tomlinson *et al.*, 2008) and antioxidant effect (Pawlak *et al.*, 2012). Studies back to 1970 and earlier have demonstrated the importance of zinc concentration in healing of thermal injuries (Henzel *et al.*, 1970). Zinc is highly important in skin (Rosten *et al.*, 2002). The skin content of zinc is a relatively high (about 5% of body content), mainly, present within the epidermis (50-70 µg/g dry weight) (Gupta *et al.*, 2014). Therefore, mild zinc deficiency can lead to impairment in wound healing (Lansdown *et al.*, 2007).

MOFs are characterized by highly porous surface area, tunable consistent pore sizes, thermal solidity, great internal capacities, no adverse effects, i.e., biocompatible, and easiness in manufacture. Therefore, they have been widely researched for application in biomedicine as drug carriers (Yu *et al.*, 2017 & 2018).

On the other hand, MOFs are getting wider application because of their rapid and economical wound healing (Yu *et al.*, 2018; Ren *et al.*, 2019; Zhang S. *et al.*, 2020). The antibacterial and anti-inflammatory effects of zinc and the physiochemical features of MOFs, make zn-based MOFs effective to overcome difficulties in wound healing. This was similar to findings reported by Chen *et al.* (2022). In another study, Zn-based metal organic framework (MOF) explored antimicrobial activity against

staphylococcus aureus (Restrepo *et al.*, 2017). The antibiotics can effectively reduce the chance of bacterial infection; however, their effectiveness getting threaten yearly due to drug-resistant bacteria (Levin-Reisman *et al.*, 2017). Zn has good biocompatibility and is easy metabolized without cumulative effect, therefore, zn-based MOF can be used as an ideal antibacterial material (Zhang *et al.*, 2013; Zhu *et al.*, 2019).

Our findings revealed that Zn-MOF positively enhanced the re-epithelization of the wound area promoting the epidermal hyperplasia that started from the wound edges toward the center leading to a reduce in the wound size and the epithelial gap that was completely closed and healed on day 21 post-wound induction. On the other side, the healing process of control wounds was at a slower rate with time leaving epithelial gaps and the wound did not entirely close on the third weeks (day 21) post-wound induction.

Zn-MOF treated wounds' dermis was pervaded with the inflammatory cells (macrophages, neutrophils,) on the first week post-wound induction which are essential for removing the dead cells, microorganisms and clean up the wound site (Ackermann, 2017; Rodrigues *et al.*, 2019). By time, there were a gradual reduction in the inflammatory cells' numbers on the second and third weeks following the induction of wounds and replaced by

fibroblasts for collagen formation. On the other side, the dermis of control wounds was severely infiltrated with a larger number of inflammatory cells and excessive hemorrhage that continued at a high level throughout the wound experiment to day 21 post-wound induction.

The new blood vessels formed in the site of wound are important during the process of healing, as they supply the wound area with, nutrients, oxygen, and immune cells. additionally, they clean up toxic waste products (Logsdon *et al.*, 2014; Honnegowda *et al.*, 2015). Zn-MOF treated wounds, had an augment in the number and size of newly formed blood vessels that facilitated the healing process in comparison to the control ones, reaching the highest point on the second week (day 14) and afterward declining on the third week (day 21) following the induction of wound with completion of the healing process. Both Zn-MOF treated and control wounds, had less collagen during the very early stage of the process of healing, on day 7 post-wound induction due to the wounds being lately inflamed and at the start of the fibroblast proliferation. Afterward, collagen deposition quantity rose obviously on the third week (day 21) after the surgical wound induction in Zn-MOF treated wounds because of maturation of connective tissue and remodeling.

CONCLUSION

Zn-MOF accelerated and enhanced the wound healing process and abundant granulation tissue formation in dogs.

REFERENCES

- Ackermann, M.R. (2017):* Inflammation and healing. In: Zachary JF, editor. Pathological basis of veterinary disease. 6th ed. St. Louis, Missouri: Elsevier; p. 73–131.
- Bhutda, S.; Surve, M.V.; Anil, A.; Kamath, K.; Singh, N.; Modi, D. and Banerjee, A. (2017):* Histochemical Staining of Collagen and Identification of Its Subtypes by Picrosirius Red Dye in Mouse Reproductive Tissues. *Bio-Protocol*, 7: e2592-e2592.
- Bielefeld, K.A.; Amini-Nik, S. and Alman, B.A. (2013):* Cutaneous wound healing: recruiting developmental pathways for regeneration. *Cell. Mol. Life Sci.* 70, 2059–2081.
- Borena, B.M.; Martens, A.; Broeckx, S.Y.; Meyer, E.; Chiers, K.; Duchateau, L. and Spaas, J.H. (2015):* Regenerative Skin wound healing in mammals: State-of-the-art on growth factor and stem cell-based treatments. *Cell. Physiol. Biochem.*, 36, 1–23.
- Chen, Y.; Cai, J.; Liu, D.; Liu, S.; Lei, D.; Zheng, L.; Wei, Q. and Gao, M. (2022):* Zinc-based metal organic framework with antibacterial and anti-inflammatory properties for promoting wound healing. *Regenerative Biomaterials*, rbac019.
- Chen, G.; Yu, Y.; Wu, X.; Wang, G.; Gu, G. and Wang, F. (2019):* Microfluidic electrospray niacin metal-organic frameworks encapsulated microcapsules for wound healing. *Research* 2019:6175398.
- Cho, J.G.; Park, S.; Lim, C.H., Kim, H.S.; Song, S.Y.; Roh, T.Y.; Sung, J.H., Suh, W.; Ham, S.J. and Lim, K.H. (2016):* ZNF224, Kruppel like zinc finger protein, induces cell growth and apoptosis-resistance by down-regulation of p21 and p53 via miR-663a. *Oncotarget*, 7, 31177–31190.
- Cronin, L. and Walton, P.H. (2003):* Synthesis and structure of [Zn (OMe)(L)] × [Zn (OH)(L)] × 2(BPh₄), L = cis, cis-1,3,5- tris [(E, E)-3-(2-furyl) acrylideneamino] cyclohexane: Structural models of carbonic anhydrase and liver alcohol dehydrogenase. *Chem. Commun. (Camb. Engl.)*, 13, 1572–1573.
- Das, S. and Baker, A.B. (2016):* Biomaterials and nanotherapeutics for enhancing skin wound healing. *Front. Bioeng. Biotechnol.* 4:82.
- Fischer, A.H.; Jacobson, K.A.; Rose, J. and Zeller, R. (2008):* Hematoxylin and Eosin Staining of Tissue and Cell Sections. *Cold*

- Spring Harbor. Protocol, (5): pdb. Prot4986.
- Gupta, M.; Mahajan, V.K.; Mehta, K.S. and Chauhan, P.S. (2014):* Zinc therapy in dermatology: A review. *Dermatol. Res. Pract.*, 709152.
- Gurtner, G.C.; Werner, S.; Barrandon, Y. and Longaker, M.T. (2008):* Wound repair and regeneration. *Nature* 453: 314–321
- Henzel, J.H.; DeWeese, M.S. and Lichti, E.L. (1970):* Zinc concentrations within healing wounds. Significance of postoperative zincuria on availability and requirements during tissue repair. *Arch. Surg.*, 100, 349–357.
- Hinks, N.J.; McKinlay, A.C.; Xiao, B.; Wheatley, P.S. and Morris, R.E. (2010):* Metal organic frameworks as NO delivery materials for biological applications. *Micropor. Mesopor. Mater.* 129, 330–334.
- Honnegowda, T.M.; Kumar, P.; Udupa, E.G.P.; Kumar, S.; Kumar, U. and Rao, P. (2015):* Role of angiogenesis and angiogenic factors in acute and chronic wound healing. *Plast Aesthet Res.* 2015; 2: 243–9.
- Hou, K. and Tang, Z. (2019):* Powerful dual metal-organic framework heterointerface for wound healing. *ACS Cent. Sci.* 5, 1488–1489.
- Hoop, M.; Walde, C.F.; Ricco, R.; Mushtaq, F.; Terzopoulou, A.; Chen, X.; Demello A. J.; Doonan, C. J.; Falcaro, P.; Nelson, B.J.; Puigmarti-Luis, J. and Pane, S. (2017):* Biocompatibility characteristics of the metal organic framework ZIF-8 for therapeutical applications. Elsevier Ltd. 2352-9407.
- Kargozar, S.; Hamzehlou, S. and Baino, F. (2019):* Can bioactive glasses be useful to accelerate the healing of epithelial tissues? *Mater. Sci. Eng. C* 97, 1009–1020.
- Karimi, K.; Odhav, A.; Kollipara, R.; Fike, J.; Stanford, C. and Hall, J.C. (2017):* Acute cutaneous necrosis: A guide to early diagnosis and treatment. *J. Cutan. Med. Surg.*, 21, 425–437.
- Kitagawa, S.; Kitaura, R. and Noro, S. (2004):* Functional porous coordination polymers. *Angew Chem Int Ed Engl.* 43: 2334–2375.
- Lansdown, A.B.; Mirastschijski, U.; Stubbs, N.; Scanlon, E. and Agren, M.S. (2007):* Zinc in wound healing: Theoretical, experimental, and clinical aspects. *Wound Repair Regen.*, 15, 2–16.
- Levin-Reisman, I.; Ronin, I.; Gefen, O.; Braniss, I.; Shores, N. and Balaban, N.Q. (2017):* Antibiotic tolerance facilitates the evolution of resistance. *Science*; 355: 826–30.
- Logsdon, E.A.; Finley, S.D.; Popel, A.S. and MacGabhann, F. (2014):* A systems biology view of blood vessel growth and remodelling. *J*

- Cell Mol Med. 2014;18: 1491–508.
- Martin, P. (1997):* Wound healing — aiming for perfect skin regeneration. *Science* 276, 75–81.
- Pawlak, K.; Mysliwiec, M. and Pawlak, D. (2012):* The alteration in Cu/Zn superoxide dismutase and adhesion molecules concentrations in diabetic patients with chronic kidney disease: The effect of dialysis treatment. *Diabetes Res. Clin. Pract.*, 98, 264–270.
- Regan, M.C. and Barbul, A. (1999):* The cellular biology of wound healing. *Wound Heal* 1:3–17.
- Ren, X.; Yang, C.; Zhang, L.; Li, S.; Shi, S. and Wang, R. (2019):* Copper metal–organic frameworks loaded on chitosan film for the efficient inhibition of bacteria and local infection therapy. *Nanoscale* 11, 11830–11838.
- Restrepo, J.; Serroukh, Z.; Morales, J.S.; Aguado, S.; Gomez-Sal, P.; Mosquera, M.E.G. and Rosal, R. (2017):* An Antibacterial Zn–MOF with Hydrazinebenzoate Linkers. *Eur. J. Inorg. Chem.*, 574–580.
- Rezwan, K.; Chen, Q.Z.; Blaker, J.J. and Boccaccini, A.R. (2006):* Biodegradable and bioactive porous polymer/inorganic composite scaffolds for bone tissue engineering. *Biomaterials*. 27: 3413–3431.
- Rodrigues, M.; Kosaric, N.; Bonham, C.A. and Gurtner, G.C. (2019):* Wound healing: a cellular
- Roohani, N.; Hurrell, R.; Kelishadi, R. and Schulin, R. (2013):* Zinc and its importance for human health: An integrative review. *J. Res. Med. Sci.*, 18, 144–157
- Rostan, E.F.; DeBuys, H.V.; Madey, D.L. and Pinnell, S.R. (2002):* Evidence supporting zinc as an important antioxidant for skin. *Int. J. Dermatol.*, 41, 606–611.
- Rubin, H.N.; Neufeld, B.H. and Reynolds, M.M. (2018):* Surface-anchored metalorganic framework-cotton material for tunable antibacterial copper delivery. *ACS Appl. Mater. Interf.* 10, 15189–15199.
- Sardari, K.; Kasemi, H.; Emami, M.R.; Movasaghi, A.R. and Goli, A.A. (2009):* Role of collagen cross-linking on equine wound contraction and healing. *Comp Clin Pathol.*, 18: 239 – 247.
- Sardari, K.; Pedram, S.; Zojaji, V.; Maleki, M.; Mohri, M.; Dehgan, M. and Emami, M.R. (2006):* effect of zn-7 on open wound healing in dogs. *Comp Clin Pathol.* 15: 237-243.
- Schiavon, M.; Francescon, M.; Drigo, D.; Salloum, G.; Baraziol, R.; Tesei, J.; Fraccalanza, E. and Barbone, F. (2016):* The Use of Integra Dermal Regeneration Template Versus Flaps for Reconstruction of Full-Thickness Scalp Defects Involving the Calvaria: A Cost-Benefit

- Analysis. *Aesthet. Plast. Surg.*, 40, 901–907.
- Singer, A.J. and Clark, R.A. (1999):* Cutaneous wound healing. *N Engl J Med* 341: 738–746.
- Soliman, E.B. (2005):* Physiological reactions and growth performance of lambs supplemented by vitamin A and zinc under summer condition. *Assiut veterinary medicine journal*, 151, No. 106.
- Suarato, G.; Bertorelli, R. and Athanassiou, A. (2018):* Borrowing from nature: Biopolymers and Biocomposites as smart wound care materials. *Frontiers in bioengineering and biotechnology*; 6, 137.
- Tomlinson, M.L.; Garcia-Morales, C.; Abu-Elmagd, M. and Wheeler, G.N. (2008):* Three matrix metalloproteinases are required in vivo for macrophage migration during embryonic development. *Mechan. Dev.*, 125, 1059–1070.
- Tottoli, E.M.; Dorati, R.; Genta, I.; Chiesa, E.; Pisani, S. and Conti, B. (2020):* skin wound healing process and new emerging technologies for skin wound care and regeneration. *Pharmaceutics*; 12,8, 735.
- Ward, J.; Holden, J.; Grob, M. and Soldin, M. (2019):* Management of wounds in the community: Five principles. *Br. J. Community Nurs.*, 24, S20–S23.
- Weller, C. and Sussman, G. (2006):* Wound dressings update. *J. Pharm. Prac. Res.* 36, 318–324.
- Xiao, J.; Chen, S.; Yi, J., Zhang, H.F. and Ameer, G.A. (2017):* A cooperative copper metal–organic framework-hydrogel system improves wound healing in diabetes. *Adv. Funct. Mater.* 27:1604872.
- Yao, X.; Zhu, G.; Zhu, P.; Ma, J.; Chen, W. and Liu, Z. (2020):* Omniphobic ZIF-8@hydrogel membrane by microfluidic-emulsion-templating method for wound healing. *Adv. Funct. Mater.* 30:1909389.
- Ye, J.; Zhao, L.; Bogale, R.F.; Gao, Y.; Wang, X.; Qian, X.; Guo, S.; Zhao, J. and Ning, G. (2015):* Highly selective detection of 2,4,6-trinitrophenol and Cu(2p) ions based on a fluorescent cadmium-pamoate metal-organic framework. *Chem Eur J.* 21: 2029–2037.
- Yu, J.; Mu, C.; Yan, B.; Qin, X.; Shen, C. and Xue, H. (2017):* Nanoparticle/MOF composites: preparations and applications. *Mater. Horiz.* 4, 557–569.
- Yu, Y.; Chen, G.; Guo, J.; Liu, Y.; Ren, J. and Kong, T. (2018):* Vitamin metal–organic framework-laden microfibers from microfluidics for wound healing. *Mater. Horiz.* 5, 1137–1142.
- Zhang, Y.; Nayak, T.R.; Hong, H. and Cai, W. (2013):* Biomedical applications of zinc oxide nanomaterials. *Curr Mol Med*; 13: 1633–45.
- Zhang, M.; Qiao, R. and Hu, J. (2020):* Engineering metal–organic

- frameworks (MOFs) for controlled delivery of physiological gaseous transmitters. *Nanomaterials* 10:1134.
- Zhang, S.; Ye, J.; Sun, Y.; Kang, J.; Liu, J. and Wang, Y. (2020):* Electrospun fibrous mat based on silver (I) metal-organic frameworks-poly(lactic acid) for bacterial killing and antibiotic-free wound dressing. *Chem. Eng. J.* 2020:124523.
- Zheng, J.; Lang, Y.; Zhang, Q.; Cui, D.; Sun, H.; Jiang, L.; Chen, Z.; Zhang, R.; Gao, Y. and Tian, W. (2015):* Structure of human MDM2 complexed with RPL11 reveals the molecular basis of p53 activation. *Genes Dev.*, 29, 1524–1534.
- Zhu, D.; Cockerill, I.; Su, Y.; Zhang, Z.; Fu, J.; Lee, K.W.; Ma, J.; Okpokwasili, C.; Tang, L.; Zheng, Y.; Qin, Y.X. and Wang, Y. (2019):* Mechanical strength, biodegradation, and in vitro and in vivo biocompatibility of Zn biomaterials. *ACS Appl Mater Interfaces*;11: 6809–19.

تقييم التئام الجروح المضمدة بأطر الزنك المعدنية العضوية في الكلاب: دراسة تجريبية

ريهام محمد عبد العظيم ، أحمد ابراهيم ، محمد حسنى قطب ، عبد النبي الشهاوى ،
سامية مصطفى سليم

E-mail: az4524311@gmail.com Assiut University web-site: www.aun.edu.eg

هدفت هذه الدراسة إلى تقييم التئام الجروح المضمدة بأطر الزنك المعدنية العضوية (zn-MOF) في الكلاب. أُجريت هذه الدراسة على خمس عشر كلباً هجيناً يتمتعون بصحة جيدة. حيث أُجري لكل كلب جرح استئصالي جلدي على كل جانب: الأيمن و الأيسر (2×2 سم²). تم تضميد جروح الجانب الأيمن بضمادة zn-MOF (الجروح المُعالجة)، بينما تم تضميد جروح الجانب الأيسر بمحلول ملحي (مجموعة التحكم). ومن ثم تم تقييم الجروح خلال الفترات التالية 7 و 14 و 21 يوماً بعد الجرح (5 كلاب في كل فترة). عززت ضمادة أطر الزنك المعدنية العضوية إعادة تكوين النسيج الجلدي لمنطقة الجرح بشكل صحي، مما أدى إلى تقليل حجم الجرح ومن ثم إغلاقه تماماً في الأسبوع الثالث بعد الجرح. كان معدل التئام مجموعة التحكم أبطأ مع مرور الوقت وتركت فجوة طلائية ولم يُغلق الجرح تماماً في الأسابيع الثلاثة الأولى بعد الجرح. انتشرت الخلايا الالتهابية داخل أدمة الجلد في اليوم السابع بعد الجرح للجروح المُعالجة ب zn-MOF، ومن ثم تقلص حجم الجرح تدريجياً مع الوقت واستبدلت الخلايا الالتهابية بخلايا ليفية في اليوم ال 14 و ال 21 يوماً بعد الجرح. بينما أدمة مجموعة التحكم امتلأت بعدد أكبر من الخلايا الالتهابية والنزيف المفرط طوال فترة الدراسة. وكذلك تم ملاحظة زيادة عدد الأوعية الدموية المتكونة في الجروح المُعالجة بأطر الزنك المعدنية العضوية مقارنةً بمجموعة التحكم، حيث وصلت إلى أعلى نقطة لها في اليوم ال 14 و انخفضت في اليوم ال 21 بعد الجرح. زاد ترسب الكولاجين بشكل واضح في اليوم ال 21 في الجروح المُعالجة بأطر الزنك المعدنية العضوية. لذلك فإن أطر الزنك المعدنية العضوية تحفز وتُسرع من عملية التئام الجروح وكذلك تكوين النسيج الحبيبي في الكلاب.

الكلمات المفتاحية: أطر الزنك المعدنية العضوية، الزنك، الكلاب، الجروح، التئام الجروح.